Journal of Electrochemistry

Volume 23 | Issue 4

2017-08-25

Density functional investigation on cathode/electrolyte interface in solid-state lithium batteries

Xuelong Wang

Ruijuan Xiao
Beijing National Laboratory for Condensed Matter Physics, Institute of Physics, Chinese Academy of Sciences, Beijing 100190, China;, rjxiao@iphy.ac.cn

Yong Xiang

Hong Li

Liquan Chen

Recommended Citation
Xuelong Wang, Ruijuan Xiao, Yong Xiang, Hong Li, Liquan Chen. Density functional investigation on cathode/electrolyte interface in solid-state lithium batteries[J]. *Journal of Electrochemistry*, 2017 , 23(4): 381-390.
DOI: 10.13208/j.electrochem.170142
Available at: https://jelectrochem.xmu.edu.cn/journal/vol23/iss4/3

DOI: 10.13208/j.electrochem.170142 **Artical ID**:1006-3471(2017)04-0381-10
Cite this: *J. Electrochem.* **2017**, *23*(4): 381-390 **Http**://electrochem.xmu.edu.cn

Density Functional Investigation on Cathode/ Electrolyte Interface in Solid-State Lithium Batteries

WANG Xue-long[1], XIAO Rui-juan[1*], XIANG Yong[2], LI Hong[1], CHEN Li-quan[1]
(1. *Beijing National Laboratory for Condensed Matter Physics, Institute of Physics, Chinese Academy of Sciences, Beijing* 100190, *China*; 2. *School of Energy Science and Engineering, University of Electronic Science and Technology of China, Chengdu*, 611731, *China*)

Abstract: The rapidly expanding application of lithium ion batteries stimulates research interest in energy storage devices with higher energy density, better safety and faster charge/discharge speed. All-solid-state lithium batteries have been considered as promising candidates because of their fewer side reactions and better safety compared with conventional lithium-ion batteries using organic liquid electrolytes. Looking for well-matched electrode/electrolyte interfaces is one of the keys to ensuring good comprehensive performance of solid-state lithium batteries. In this report, with the aid of first-principles simulations, the local structures, lithium ions transportation properties of electrolyte surfaces and cathode/electrolyte interfaces are investigated. The β-Li_3PS_4(010) /$LiCoO_2$(104) and Li_4GeS_4(010)/$LiCoO_2$(104) interfaces are adopted as model systems to understand the bonding interaction and Li^+ migration barriers at interfaces. The ability of Li^+ motion is improved in partial delithiated state for both systems, due to that Co atoms at the interface in high oxidized state oxidize the S atoms nearby and weaken the P/Ge-S bond, resulting in less constrains on Li ions in neighbor and promoting the exchange of Li ions across the interface. It provides information for cathode/electrolyte interface optimization, and may assist to discover appropriate techniques for solid-state lithium batteries.

Key words: solid state lithium batteries; cathode/electrolyte interface; density functional theory calculations; lithium migration
CLC Number: G633.7; O646 **Document Code**: A

Advanced cell technology is the world's leading competition in the next decades. Lithium ion batteries (LIBs) are the key to the success of portable electronic products[1], electrical vehicles[2] and the best choice for the energy storage devices of wind and solar power[3] because of their high voltage, high specific energy density, rapid recharge capability, and wide working temperature range. However, the liquid electrolytes used in current LIBs contain flammable organic solvents, leading to such problems as leakage, vaporization, decomposition and safety[4]. One type of proposed next generation batteries is all-solid-state batteries, which are composed of both solid electrodes and solid electrolytes[5]. Different from the traditional LIBs with liquid electrolytes, the electrode/electrolyte interface in all-solid-state batteries is between solid and solid, thus the discovery of well-matched electrode and electrolyte is of great importance to ensure the good comprehensive performance of the batteries[6]. The electrode/electrolyte interface with high chemical stability, mechanical stability and fast lithium ionic conduction is the prerequisite for developing all-solid-state lithium secondary batteries[7]. So far, the highest lithium ion conduction achieved in solid inorganics has been found in sulfide materials, which have been established as a promising family of solid electrolytes[8]. Recently, a series of discoveries in Li super ionic conductors $Li_{10}MX_2S_{12}$ (M = Ge, Sn,. . .; X = P, Si,. . .) with lithium ion conductivity values in the order of 10^{-2} S·cm^{-1} at room temperature have been reported[9-10]. These structures can be regarded as solid solutions of the pseudo binary Li_3PS_4-Li_4GeS_4 system, which is part of the thio-LISICON family[11]. As the typical ternary compounds in Li-Ge-P-S sys-

Received: 2017-01-05, Revised: 2017-02-28 *Corresponding author, Tel: (86-10)82649845, E-mail: rjxiao@iphy.ac.cn

tem, Li_3PS_4 and Li_4GeS_4 also show good ionic conductivities[12-13]. For the cathodes, $LiCoO_2$ is the most widely used material for commercial lithium batteries due to its excellent electrochemical cycling stability[14]. To understand the interactions between electrolyte and positive electrode, we studied the interfaces of Li_3PS_4 and Li_4GeS_4 against $LiCoO_2$. In this report, with the aid of first-principles density function theory (DFT) computations, the lo cal structures, and ionic transport properties of $Li_3PS_4/LiCoO_2$ and $Li_4GeS_4/LiCoO_2$ interfaces are investigated. The bonding between Co and S is found at the interface, and the interfacial resistivity varies during the lithiation/delithiation cycling because of the varied lithium concentration near the interface. The studies will deepen the understanding on the cathode/electrolyte interfaces from the point of view of local structures, and may assist to discover appropriate techniques for electrode/electrolyte interface optimization.

1 Methods

The DFT calculations performed in this study are conducted with the Vienna ab initio simulation package (VASP)[15] within the projector augmented-wave (PAW) approach[16]. The generalized gradient approximation is adopted in the parameterization of Perdew, Burke, and Ernzerhof (PBE)[17] to describe the exchange-correlation function. For all calculations the cutoffs of wave function and charge density are 500 and 756 eV, respectively. The k-mesh used to sample the Brillouin zone is in the density of one point per 0.05 $Å^{-3}$. Both ions and cells are relaxed in the optimization with the energy and force convergence criterion of 10^{-5} eV and 0.01 eV · $Å^{-1}$, respectively. The models used for the simulation of surface structure consist of slabs cut out of crystalline structure along the surface of interests and an extra 20 Å thick vacuum to exclude interactions between periodic slab images. The model for the simulation of interface structure is built by periodically arranging electrolyte and electrode slabs. The slabs used in surface and inter face simulations contain 12 formula units (f.u.) of Li_3PS_4, 12 f.u. of Li_4GeS_4 and 11 f.u. of $LiCoO_2$ respectively. The BV method[18-20] is employed to obtain a direct visualization of the Li migration pathways and provides reference on throughout activation energies for Li ions moving.

2 Results and Discussion

2.1 Crystal Structure and Li Transport in Bulk

To establish a well-defined cathode/electrolyte interface model, it is vital to acquire well optimized crystal structures and understand the ionic transport features in the bulk region in first place. We conduct the DFT-based first principles relaxation for the crystal structures of β-Li_3PS_4, Li_4GeS_4 and $LiCoO_2$. The resulting lattice parameters are listed in Table 1 together with the previously measured values from the experiments[21-23]. As can be seen from Table 1, the optimized lattice constants ***a***, ***b*** and ***c*** fit well with the ones from experiments with differences no bigger than 2%. The shapes and symmetry of the cells stay unchanged as described by the same space group characterized by experimental methods.

The transportation of Li ions is the other issue of the most interests. To get an intuitive impression of the migration channels, we adopt a semi-empirical BV-based force-field method code package, BV path[24], to evaluate the transport feature of Li ions in different materials. This method has been proved to be efficient in predicting ionic transportation pathways[18-19] and offering a valuable reference on throughout activation energies in highly consistence with the ones from accurate DFT calculations[20]. The migration paths of Li ions simulated by BV path code for crystalline β-Li_3PS_4, Li_4GeS_4 and $LiCoO_2$ are shown in Fig. 1. The continuous pathways for Li ion (Li^+) migration are indicated by the enclosed yellow isosurfaces. The isovalues for getting these enclosed isosurfaces are 0.85 eV, 1.255 eV and 1.81 eV for β-Li_3PS_4, Li_4GeS_4 and $LiCoO_2$ respectively, giving the trend in the ability of Li^+ motion consistent with quantum mechanical sim ulations[25-28]. For solid electrolyte materials β-Li_3PS_4 and Li_4GeS_4, the views along ***b*** and ***c*** axes are provid ed and for $LiCoO_2$ the views along [210] direction and ***b*** axis are shown. The resemblance between the Li^+ migration paths in β-Li_3PS_4 and that in Li_4GeS_4 are

Tab. 1 Calculated lattice parameters for β-Li_3PS_4, Li_4GeS_4 and $LiCoO_2$. Experimental data are listed for comparison.

	β-Li_3PS_4		Li_4GeS_4		$LiCoO_2$	
Space group	Cal.	Exp.[1]	Cal.	Exp.[2]	Cal.	Exp.[3]
	Pnma	Pnma	Pnma	Pnma	R-3mH	R-3mH
a [Å]	13.0980	12.8190	14.1464	14.0340	2.8586	2.8155
b [Å]	8.1328	8.2195	7.8344	7.7548	2.8586	2.8155
c [Å]	6.2567	6.1236	6.2138	6.1502	14.0393	14.0497
α [°]	90	90	90	90	90	90
β [°]	90	90	90	90	90	90
γ [°]	90	90	90	90	120	120

quite obvious for that both channels are running throughout the lattice in two-dimensional (2D) ***bc*** plane, suggesting a 2D-like transport behavior of Li ions in these materials, which is consistent with the results from previous studies[25-26]. Actually, the crystal structures of β-Li_3PS_4 and Li_4GeS_4 are indeed very much alike as both consist of mobile Li ions and a steady host framework formed by P/GeS_4 tetrahedrons in the same positional arrangement. However, slight differences between these two structures still exist rooted in the fact that P and Ge are in different valence states having different ionic radii. These differences cause little shrinkages of ***b*** and ***c***, and elongation of ***a*** in Li_4GeS_4 as compared to β-Li_3PS_4 which results in compressed space inside a GeS_4 tetrahedron layer and more free space between the layer. Therefore, compared with the situation in β-Li_3PS_4 the migration channels of Li ions in Li_4GeS_4 are less constrained to a 2D layer, while have a tendency to form an interlayer connection showing a bit 3D transportation feature. On the other hand, the migration paths of Li ions in $LiCoO_2$ show a significant 2D feature only existing inside the LiO_6 layer and the hopping path between one octahedron center and another passes a tetrahedron center suggested by the interstitial hollow sphere at the tetrahedron center connecting two adjacent octahedron sites. These features of the migration channel fit well with conclusions of many studies on layered transition metal oxides[27-28]. The much dispersed potential isosurface and much smaller isovalue of it in solid electrolyte materials (SEs) than those in electrode reflects the fact that ionic conductivity in SEs is better than in electrode. However, the 2D-like transportation behavior in all three materials poses another requirement on assembling these materials that the interface should intersect with these transporting planes to lower the interface ionic resistance. Taking this into consideration we conduct the relaxation of these three surfaces described in detail in section 2.2.

2.2 Surface Structure

Out of the consideration of exposing the ionic transportation channel to the surface we chose slabs with the β-Li_3PS_4(010), Li_4GeS_4(010) and $LiCoO_2$ (104) surfaces as three modelling systems. The (104) surface of $LiCoO_2$ was also observed existing in experiment[29]. An extra 20 Å vacuum layer is added on each of the slabs to avoid unnecessary interactions between periodical slab images and the relaxed slab structures are shown in Fig. 2. As can be seen from the figures, in the middle layer of all three slabs the structure stays identical to the crystalline structure which indicates a well recovered bulk region in the slab models we adopt. For the surface region a slight distortion of host tetrahedrons is observed in two electrolyte materials, while no obvious distortion of polyhedrons is seen in the situation of $LiCoO_2$ in spite of the incomplete CoO_6 octahedron with one O atom missing on the (104) surface. In general no significant surface reconstruction is found on these three surfaces.

2.3 Interface Property

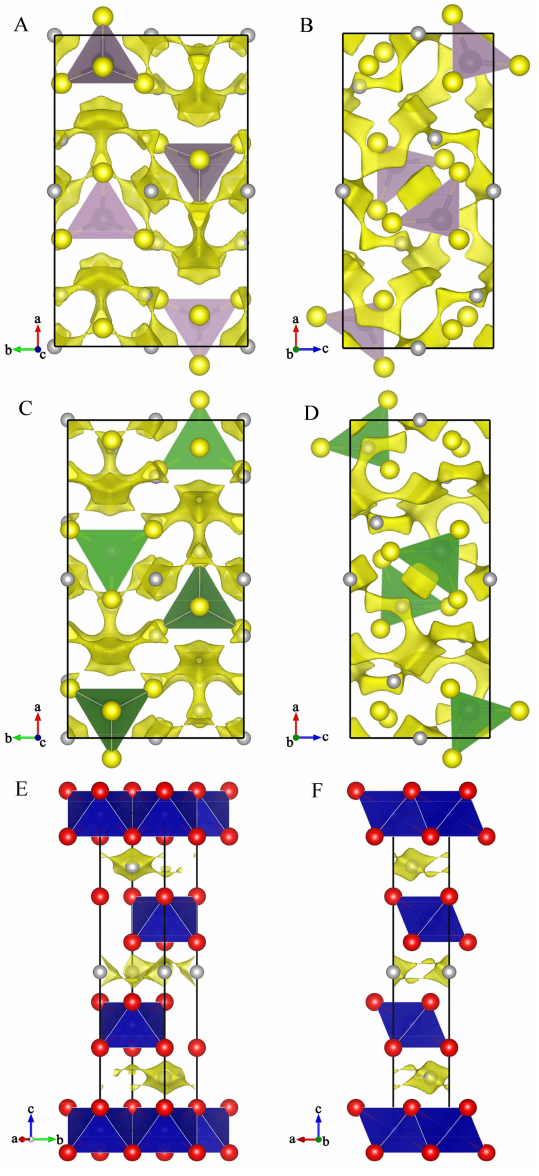

Fig. 1 The lithium migration pathways revealed by BV-based method for β-Li_3PS_4 (A) viewed along ***c*** axis, β-Li_3PS_4 viewed along ***b*** axis (B), Li_4GeS_4 viewed along ***c*** axis (C), Li_4GeS_4 viewed along ***b*** axis (D), $LiCoO_2$ viewed along [210] direction (E) and $LiCoO_2$ viewed along ***b*** axis (F). The isosurfaces used to present the paths are obtained with the isovalues of 0.85 eV, 1.255 eV and 1.81 eV for β-Li_3PS_4, Li_4GeS_4 and $LiCoO_2$ respectively. The white, red and yellow bullets represent Li, O and S, respectively, while grey, green and blue polyhedrons represent PS_4, GeS_4 and CoO_6 units, respectively.

To build the proper interface model the compatibility between two surfaces is carefully considered in our studies. A 2D supercell in $LiCoO_2$(104) surface is constructed to minimize the deviation between the lattice parameters of cathode material and electrolyte material. All atomic configurations with inequivalent relative positions of two surfaces are generated by translating and rotating slabs with $LiCoO_2$ (104) surface in the plane parallel to the interface and 41 different configurations are considered in total. The configuration with lowest total energy is chosen as the ground state structure and further optimization is conducted upon it. In both β-Li_3PS_4(010)/$LiCoO_2$ (104) and Li_4GeS_4(010)/$LiCoO_2$(104) systems, the situations where $LiCoO_2$ is delithiated are also evaluated. The Li ions in the two layers closest to the interface are removed to simulate the condition when the cell is partially charged. The atomic structures and the ionic transportation features at these interfaces are discussed in detail in the following paragraphs.

1) β-Li_3PS_4(010)/$LiCoO_2$(104) Interface

The relaxed structure and the Li ionic transportation channel simulated by BV path code for interface of Li_3PS_4(010) slab with pristine $LiCoO_2$ and delithiated $LiCoO_2$(104) slab are shown in Fig. 3 and Fig. 4, respectively. The atomic configuration of ground state is found to be (104) surface of $LiCoO_2$ rotating a certain angle relative to the (010) surface of β-Li_3PS_4. As can be seen from the picture, $LiCoO_2$ being delithiated or not, the middle region of the slab preserves the crystalline structure, while distortion of polyhedrons happens mostly at the interface region. When no lithium is removed from $LiCoO_2$ only one Co atom on the (104) surface in the supercell bonds with sulfur from β-Li_3PS_4, while in the delithiated state every Co atom on the (104) surface bonds with the sulfur atom on the surface of β-Li_3PS_4 causing severe distortion of PS_4 tetrahedrons. This difference can be understood since the Co atoms on surface are in higher oxidation state when some Li ions are removed and have stronger interactions with anions in electrolyte. However, this interaction between Co and S at the interface benefits the Li ion transportation through the interface. The minimal energy needed to connect the migration channel in delithiated $LiCoO_2$ and β-Li_3PS_4 is 1.43 eV, smaller than 1.75 eV in the

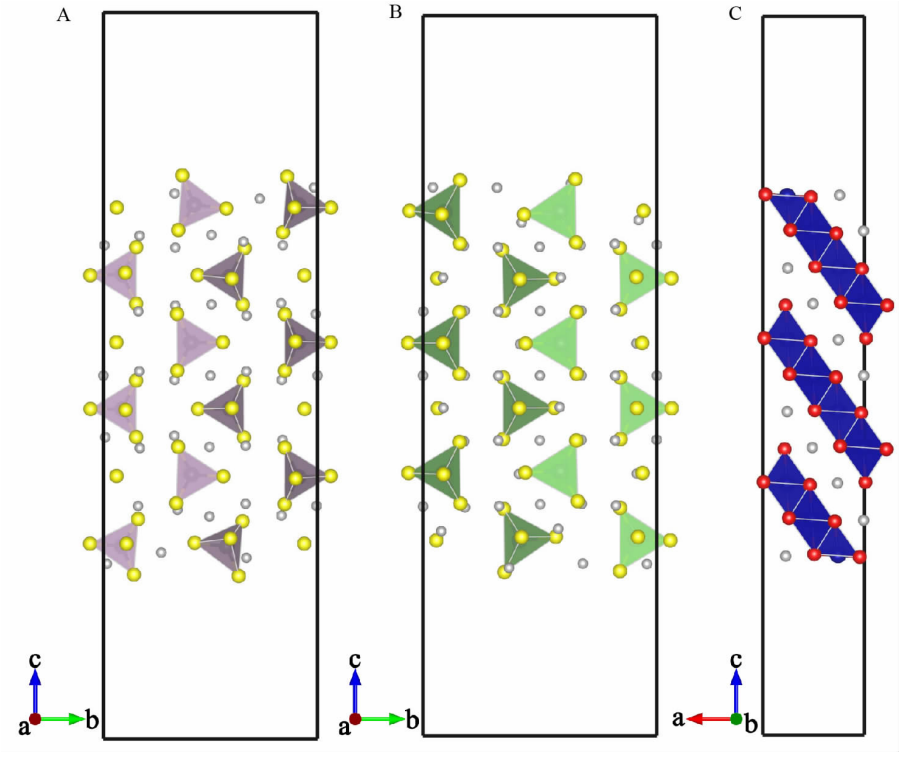

Fig. 2 The relaxed structures for β-Li_3PS_4(010) (A), Li_4GeS_4(010) (B) and $LiCoO_2$(104) (C) surfaces. The white, red and yellow bullets represent Li, O and S, respectively, while grey, green and blue polyhedrons represent PS_4, GeS_4 and CoO_6 units, respectively.

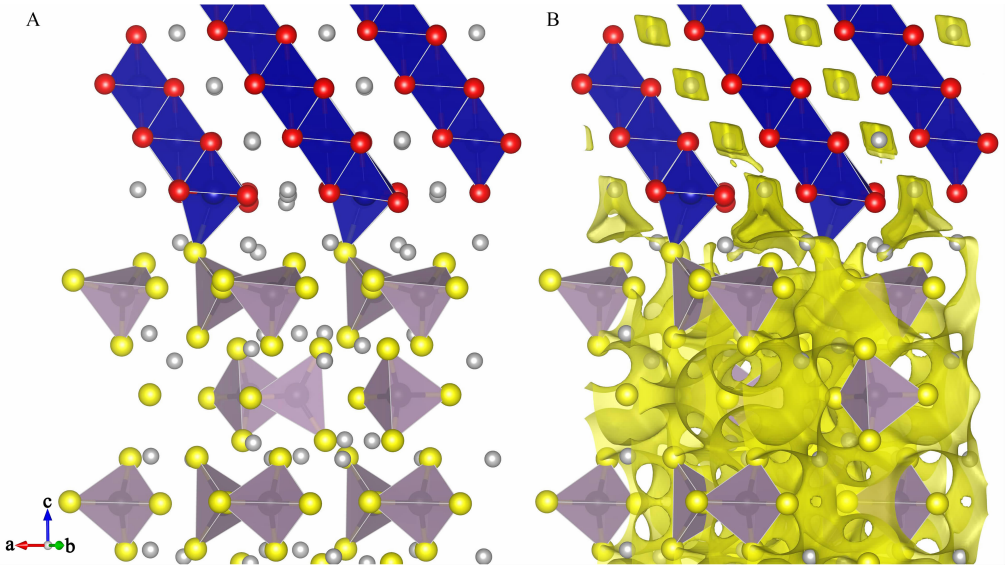

Fig. 3 The relaxed atomic structure for β-Li_3PS_4(010)/$LiCoO_2$(104) interface (A), and the lithium migration pathways at the interface revealed by BV-based method (B). The isosurfaces used to present the paths are obtained with the isovalues of 1.75 eV. The white, red and yellow bullets represent Li, O and S, respectively. Grey and blue polyhedrons represent PS_4 and CoO_6 units, respectively.

situation without Li ions removed. It can be speculated that at this level of delithiation with about one third of Li ions pulled out from $LiCoO_2$ the Li ions travel easier between cathode and electrolyte. Actual-

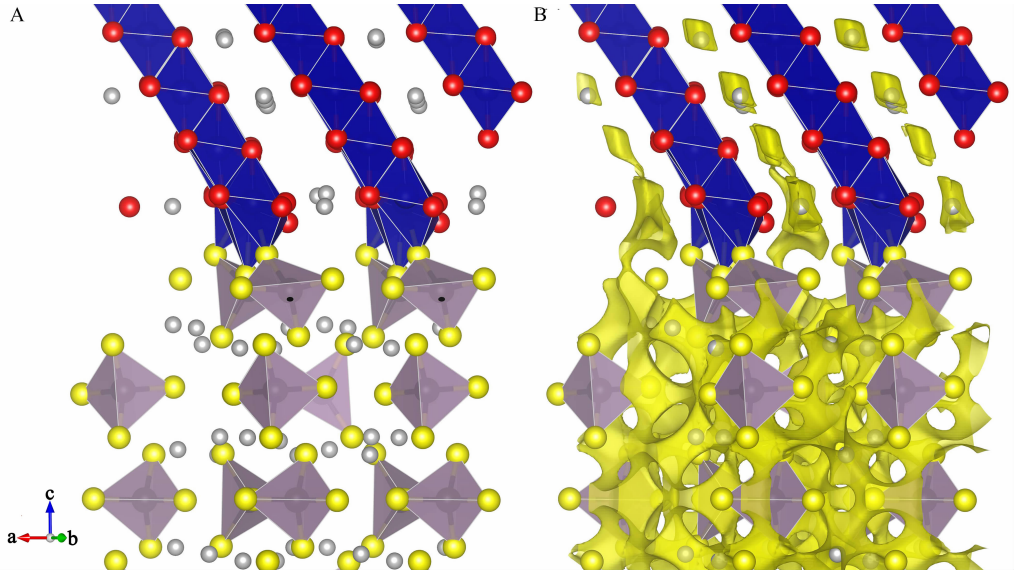

Fig. 4 The relaxed atomic structure for β-Li_3PS_4(010)/$Li_{0.64}CoO_2$(104) interface (A), and the lithium migration pathways at the interface revealed by BV-based method (B). The isosurfaces used to present the paths are obtained with the isovalues of 1.43 eV. The white, red and yellow bullets represent Li, O and S, respectively. Grey and blue polyhedrons represent PS_4 and CoO_6 units, respectively.

ly, this kind of Co-S bonds formed at the interface between $LiCoO_2$ and β-Li_3PS_4 has been found by first principles simulation before[30-31] only where the situation was with $LiCoO_2$(110) surface. Slight Li ions accumulation at the interface was also found together with Co-S bond in the previous study which is partly in accordance with our results that the ionic migration channel is more enlarged at the interface compared with that in the bulk region of $LiCoO_2$. However, since the BV method only takes static interaction potential into account in simulating ionic pathways the effects of space charge layer mentioned in the previous study do not reflect on our results. If we inspect the bonds formed at the interface it would be found that P-S bond is stretched after S bonding with Co. When no Li is extracted the P-S bond is stretched a little bit to 2.067 Å compared to 2.055 Å in bulk region. However, when some Li ions are removed from $LiCoO_2$, the P-S bond in the distorted tetrahedron is stretched a lot to 2.281 Å, and this means that Co in the near neighbor weakens the P-S bond and partially oxidize the S^{2-} ion which would weaken the constrains on Li ions nearby as a by-product.

2) Li_4GeS_4(010)/$LiCoO_2$(104) Interface

The relaxed structure and transportation channel for Li_4GeS_4(010)/$LiCoO_2$(104) interface are shown in Fig. 5 and Fig. 6. Different from the situation with β-Li_3PS_4, no rotation of $LiCoO_2$ (104) surface is found in the atomic configuration with lowest total energy. This may have something to do with the different lattice parameters of Li_4GeS_4. Still the middle region of the slab preserves the crystalline structure and distortion happens mostly at the interface region. One major difference in the interface structure compared to β-Li_3PS_4(010)/$LiCoO_2$(104) is that the newly formed Co-S bonds do not change much when $LiCoO_2$ is partially delithiated, which should be credited by the positional arrangement of $LiCoO_2$(104) surface on Li_4GeS_4 being different from condition with β-Li_3PS_4. In the ground structure of Li_4GeS_4(010)/$LiCoO_2$(104) interface the Co atom on the outermost locates right on top of S atom and bond is easily formed between them even when $LiCoO_2$ is fully lithiated. Therefore, the interface structure stays almost the same after Li ions being removed from $LiCoO_2$ except for some interface Li ions changing positions. As a consequence the migration channel of Li ions through the interface do not change much either. The minimal energy

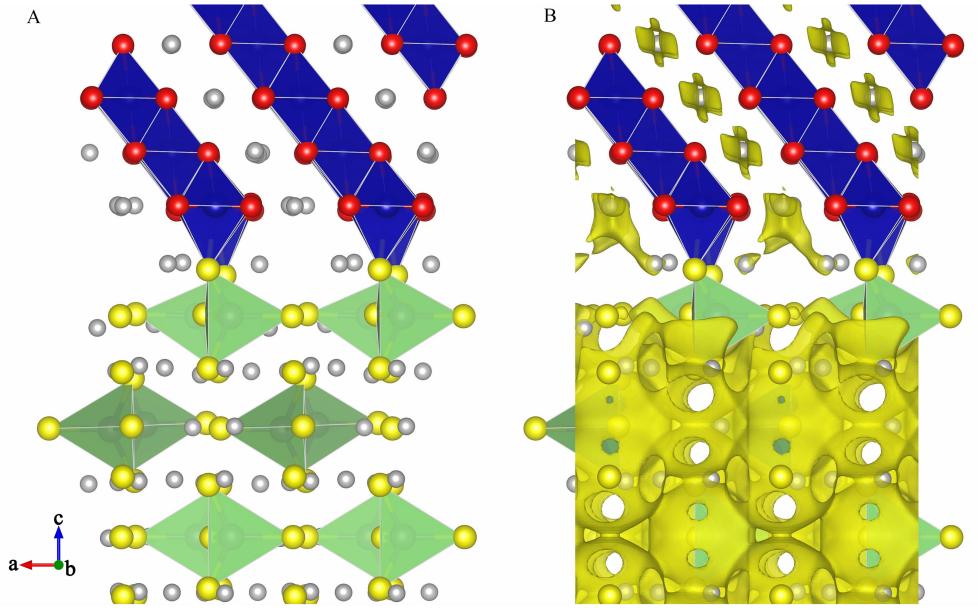

Fig. 5 The relaxed atomic structure for $Li_4GeS_4(010)/LiCoO_2(104)$ interface (A), and the lithium migration pathways at the interface revealed by BV-based method (B). The isosurfaces used to present the paths are obtained with the isovalues of 2.13 eV. The white, red and yellow bullets represent Li, O and S, respectively. Green and blue polyhedrons represent GeS_4 and CoO_6 units, respectively.

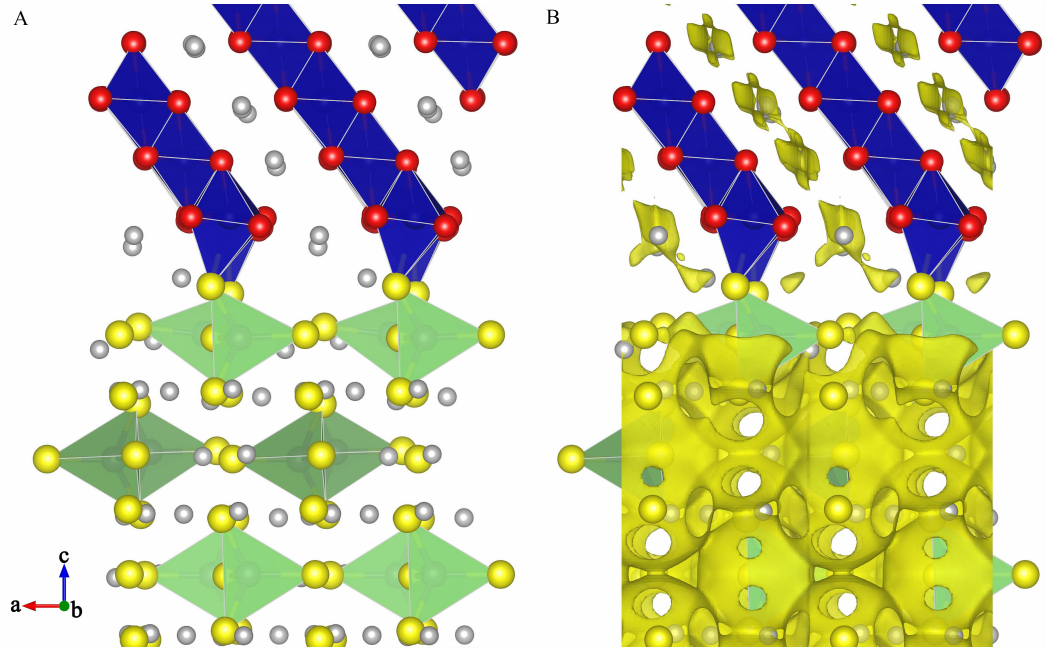

Fig. 6 The relaxed atomic structure for $Li_4GeS_4(010)/Li_{0.64}CoO_2(104)$ interface (A), and the lithium migration pathways at the interface revealed by BV-based method (B). The isosurfaces used to present the paths are obtained with the isovalues of 2.01 eV. The white, red and yellow bullets represent Li, O and S, respectively. Green and blue polyhedrons represent GeS_4 and CoO_6 units, respectively.

needed to connect the migration channel in delithiated $LiCoO_2$ and Li_4GeS_4 is 2.01 eV, while 2.13 eV for situation with all Li ions presented. It still gets a little easier for Li ions travelling between $LiCoO_2$ and Li_4GeS_4 in delithiated state though not that much as Li_3PS_4. We also inspect the bond at the interface. The

Ge-S bond in the tetrahedron sharing S atom with Co is also stretched a little compared to that in the bulk region. The averaged lengths of Ge-S bond at interface are 2.247 Å and 2.273 Å for lithiated and delithiated situations, respectively, compared to 2.244 Å in bulk region. At the same time the averaged lengths of Co-S bond at interface are 2.305 Å and 2.241 Å for lithiated and delithiated situations, respectively. These changes suggest that when some Li ions are extracted from $LiCoO_2$, Co-S bond gets stronger weakening Ge-S bond, and this competence between Co and Ge makes S^{2-} oxidized to some extent loosening the constrains on Li ions nearby and promotes the traveling abilities of them. Unlike the situation with β-Li_3PS_4, this change in bond length is not that significant which may explain that the enhancement is not as big as that in condition with Li_3PS_4.

3 Conclusions

With the aid of DFT based structure optimization and semi-empirical BV-based ionic transport simulations, the features of Li ions migration through cathode/electrolyte interface are studied, specifically exemplified by the investigations of β-Li_3PS_4(010)/$LiCoO_2$(104) and Li_4GeS_4(010)/$LiCoO_2$(104) interface systems. Through the simulations of crystalline material, the 2D-like Li ionic transportation behaviors in β-Li_3PS_4 and $LiCoO_2$ are reproduced. Surface structure optimization shows no obvious reconstruct ions of β-Li_3PS_4(010), Li_4GeS_4(010) and $LiCoO_2$(104) surfaces. By comparing the Li ions migration across the interface of electrolyte with fully lithiated and partially delithiated cathode, the change of Li ions mobility as Li ions being extracted from $LiCoO_2$ is revealed. In general it gets easier for Li ions to travel through the electrolyte/$LiCoO_2$(104) interface when $LiCoO_2$ is partially delithiated due to that Co atoms at the interface in high oxidized state oxidize the S atoms nearby and weaken the P/Ge-S bond, resulting in less constrains on Li ions in neighbor and promoting the exchange of Li ions across the interface. However, what must be addressed is that the results shown here are all based on simulation of static structure. In a dynamic process like the charging process of battery, extra side reactions may occur due to the presence of very chemically active Co atoms in high oxidized state. When new interphases are formed in a practical battery the transportation behavior of Li ions across the interface may deviate from the results provided in this work. But still these results provide information for cathode/electrolyte interface optimization, and will be conducive to build well-matched cathode/electrolyte interfaces in solid-state lithium batteries.

Acknowledgement

This work was supported by the National Natural Science Foundation of China (Grants No. 11234013), "863" Project (Grant No. 2015AA034201), Beijing S&T Project (Grant No. D161100002416003), and Youth Innovation Promotion Association (Grant No. 2016005) for financial support and the Shanghai Supercomputer Center for providing computing resources.

References:

[1] Tarascon J M, Armand M. Issues and challenges facing rechargeable lithium batteries[J]. Nature, 2001, 414(6861): 359-367.

[2] Karden E, Ploumen S, Fricke B, et al. Energy storage devices for future hybrid electric vehicles[J]. Journal of Power Sources, 2007, 168(1): 2-11.

[3] Dunn B, Kamath H, Tarascon J M. Electrical energy storage for the grid: A battery of choices[J]. Science, 2011, 334 (6058): 928-935.

[4] Xu K. Nonaqueous liquid electrolytes for lithium-based rechargeable batteries[J]. Chemical Review, 2004, 104(10): 4303-4417.

[5] Takada K. Progress and prospective of solid-state lithium batteries[J]. Acta Materialia, 2013, 61(3): 759-770.

[6] Santhanagopalan D, Qian D, McGilvray T, et al. Interface limited lithium transport in solid-state batteries[J]. Journal of Physical Chemistry Letters, 2014, 5(2): 298-303.

[7] Richards W D, Miara L J, Wang Y, et al. Interface stability in solid-state batteries[J]. Chemistry of Materials, 2016, 28 (1): 266-273.

[8] Kamaya N, Homma K, Yamakawa Y, et al. A lithium superionic conductor[J]. Nature Materials, 2011, 10(9): 682-686.

[9] Bron P, Johansson S, Zick K, et al. $Li_{10}SnP_2S_{12}$: An affordable lithium superionic conductor[J]. Journal of the American Chemical Society, 2013, 135(42): 15694-15697.

[10] Ong S P, Mo Y, Richards W D, et al. Phase stability,

electr ochemical stabil ity and ionic conductivity of the $Li_{10\pm1}MP_2X_{12}$ (M = Ge, Si, Sn, Al or P, and X = O, S or Se) family of superionic conductors[J]. Energy & Environmental Science, 2013, 6(1): 148-156.

[11] Murayama M, Sonoyama N, Yamada A, et al. Material design of new lithium ionic conductor, thio-LISICON, in the Li_2S-P_2S_5 system[J]. Solid State Ionics, 2004, 170(3/4): 173-180.

[12] Liu Z, Fu W, Payzant E A, et al. Anomalous high ionic conductivity of nanoporous β-Li_3PS_4[J]. Journal of the American Chemical Society, 2013, 135(3): 975-978.

[13] Ito Y, Sakuda A, Ohtomo T, et al. Li_4GeS_4-Li_3PS_4 electrolyte thin films with highly ion-conductive crystals prepared by pulsed laser deposition[J]. Journal of the Ceramic Society of Japan, 2014, 122(1425): 341-345.

[14] Li H, Wang Z X, Chen L Q, et al. Research on advanced materials for Li-ion batteries[J]. Advanced Materials, 2009, 21(45): 4593-4607.

[15] Kresse G, Furthmüller J. Efficiency of ab-initio total energy calculations for metals and semiconductors using a plane-wave basis set[J]. Computational Materials Science, 1996, 6(1): 15-50.

[16] Blöchl P E. Projector augmented-wave method[J]. Physical Review B, 1994, 50(24): 17953-17979.

[17] Perdew J P, Burke K, Ernzerhof M. Generalized gradient approximation made simple[J]. Physical Review Letters, 1996, 77(18): 3865-3868.

[18] Adams S, Rao R P. High power lithium ion battery materials by computational design[J]. Physica Status Solidi A, 2011, 208(8): 1746-1753.

[19] Adams S, Rao R P. Transport pathways for mobile ions in disordered solids from the analysis of energy-scaled bond-valence mismatch landscapes[J]. Physical Chemistry Chemical Physics, 2009, 11(17): 3210-3216.

[20] Xiao R J, Li H, Chen L Q. Candidate structures for inorganic lithium solid-state electrolytes identified by high-throughput bond-valence calculations[J]. Journal of Materiomics, 2015, 1(4): 325-332.

[21] Homma K, Yonemura M, Kobayashi T, et al. Crystal structure and phase transitions of the lithium ionic conductor Li_3PS_4[J]. Solid State Ionics, 2011, 182(1): 53-58.

[22] Murayama M, Kanno R, Kawamoto Y, et al. Structure of the thio-LISICON, Li_4GeS_4[J]. Solid State Ionics, 2002, 154(SI): 789-794.

[23] Antaya M, Cearns K, Preston J S, et al. *In situ* growth of layered, spinel and rock-salt $LiCoO_2$ by laser ablation deposition[J]. Journal of Applied Physics, 1994, 76(5): 2799-2806.

[24] Xiao R J, Li H, Chen L Q. High-throughput design and optimization of fast lithium ion conductors by the combination of bond-valence method and density functional theory[J]. Scientific Reports, 2015, 5: 14227.

[25] Lepley N D, Holzwarth N A W, Du Y A. Structures, Li^+ mobilities, and interfacial properties of solid electrolytes Li_3PS_4 and Li_3PO_4 from first principles[J]. Physical Review B, 2013, 88(10): 104103.

[26] Wang X L, Xiao R J, Li H, et al. Oxygen-driven transition from two-dimensional to three-dimensional transport behaviour in β-Li_3PS_4 electrolyte[J]. Physical Chemistry Chemical Physics, 2016, 18(31): 21269-21277.

[27] Kramer D, Ceder G. Tailoring the morphology of $LiCoO_2$: A first principles study[J]. Chemistry of Materials, 2009, 21(16): 3799-809.

[28] Ning F H, Li S, Xu B, et al. Strain tuned Li diffusion in $LiCoO_2$ material for Li ion batteries: A first principles study[J]. Solid State Ionics, 2014, 263: 46-48.

[29] Batesa J B, Dudneya N J, Neudeckera B J, et al. Preferred orientation of polycrystalline $LiCoO_2$ films[J]. Journal of the Electrochemical Society, 2000, 147(1): 59-70.

[30] Haruyama J, Sodeyama K, Han L, et al. Space-charge layer effect at interface between oxide cathode and sulfide electrolyte in all-solid-state lithium-ion battery[J]. Chemistry of Materials, 2014, 26(14): 4248-4255.

[31] Haruyama J, Sodeyama K, Tateyama Y. Cation mixing properties toward co diffusion at the $LiCoO_2$ cathode/sulfide electrolyte interface in a solid-state battery[J]. ACS Applied Materials & Interfaces, 2017, 9(1): 286-292.

固态锂电池中正极/电解质界面的密度泛函计算研究

王雪龙[1],肖睿娟[1*],向 勇[2],李 泓[1],陈立泉[1]
(1. 北京凝聚态物理国家实验室, 中国科学院物理研究所, 北京 100190;
2. 电子科技大学能源科学与工程学院, 四川 成都 611731)

摘要: 锂离子电池的广泛应用对储能器件的能量密度、安全性和充放电速度提出了新的要求. 全固态锂电池与传统锂离子电池相比具有更少的副反应和更高的安全性, 已成为下一代储能器件的首选. 构建匹配的电极/电解质界面是在全固态锂电池中获得优异综合性能的关键. 本文采用第一性原理计算研究了固态电池中电解质表面及正极/电解质界面的局域结构和锂离子输运性质. 选取 β-Li_3PS_4(010)/$LiCoO_2$(104)和 Li_4GeS_4(010)/$LiCoO_2$(104)体系计算了界面处的成键情况及锂离子的迁移势垒. 部分脱锂态的正极/电解质界面上由于 Co-S 成键的加强削弱了 P/Ge-S 键的强度,降低了对 Li^+ 的束缚,从而导致了更低的锂离子迁移势垒. 理解界面局域结构及其对 Li^+ 输运性质的影响将有助于人们在固态电池中构建性能优异的电极/电解质界面.

关键词: 固态锂电池; 正极/电解质界面; 密度泛函模拟; 锂离子迁移